Electronic Supplementary Material (ESI) for Journal of Materials Chemistry A.

Supporting Information

Boosting Photocatalytic CO_2 Conversion Efficiency of MOFs by Solid Electron Conveyor

Xiaofei Gu [a], Tianyi Huang [a], Yixin Hong [a], Yafeng Wu [a], Zhi Wang [c], Yuanjian Zhang [a], Songqin Liu [a, *], Jianyu Han [b, *]

[a] *Jiangsu Engineering Laboratory of Smart Carbon-Rich Materials and Device, School of Chemistry and Chemical Engineering, Medical School, Southeast University, Nanjing 211189, China.*

[b] *School of Energy and Environment, Southeast University, Nanjing 210096, China.*

[c] *Wuxi Institute of Inspection, Testing and Certification, Wuxi 214125, China.*

Experimental section

Materials

Formate dehydrogenase from C. boidinii (FDH, EC 1.2.1.2) was purchased from Shanghai Chaoyan Biotechnology Co., Ltd. 10-bromodecanoic acid, iodomethane, 4,4'-dipyridyl, zirconyl chloride octahydrate ($ZrOCl_2 \cdot 8H_2O$), 4-ethynylbenzaldehyde, ethyl 4-iodobenzoate, bis(triphenylphosphine) palladium (II) dichloride, cuprous iodide (CuI), pyrrole and 5-Carboxyfluorescein N-succinimidyl ester (FITC) were received from Aladdin (Shanghai, China). FITC-labeled FDH was synthesized through amide bond (Supporting Information). Acetone, acetonitrile, triethylamine, hexane, ethyl acetate, propionic acid, methanol (CH_3OH), potassium hydroxide (KOH), trifluoroacetate (TFA), tetrahydrofuran (THF), concentrated hydrochloric acid (HCl), dichloromethane (CH_2Cl_2), N, N-dimethylformamide (DMF), triethanolamine (TEOA) and anhydrous magnesium sulfate were purchased from Ling-Feng (Shanghai, China). Tris-HCl buffer solution (0.05 M) was prepared by adjusting pH to 7 with HCl. True choline esterase (T-CHE) was obtained from KeyGEN Biotech (Nanjing, China). All the reagents were used as received without further purification. Deionized water was prepared using a Milli-Q purification system with a resistivity of 18.2 MΩ.

Instrument

^{1}H-NMR spectra were collected from a Bruker 600 MHz spectrometer (Bruker, German). Absorbance measurement was performed by a 2450 UV-visible spectrophotometer (Shimadzu, Japan). Fluorescence (FL) spectra were carried out on a FluoroMax-4 spectrofluorometer with xenon discharge lamp excitation (HORIBA, USA). FT-IR experiments were measured on a Nicolet 4700 Fourier infrared spectrometer (Thermo, USA) equipped with an attenuated total reflection setup. The morphology of NU-1006 was characterized using scanning electron microscopy (SEM, FEI Inspect F50, USA) and corresponding EDX elemental mapping images were obtained by using a JEOL model JEM 2100 (Japan). Small angle X-ray diffraction (SAXRD) patterns of NU-1006 and CNMV-NU-1006 were recorded by a Rigaku Ultima IV X-ray diffractometer (Japan). X-ray photoelectron spectroscopy was carried out with Thermo ESCALAB 250XI (Thermo Scientific, USA), performed with Al Kα radiation (λ = 0.8339 nm). The Electron Paramagnetic Resonance (EPR) measurement was performed on a Bruker A300 system at room temperature (Bruker, German). Gas ad/desorption measurement was performed in the Quantachrome NOVA4000 System

(Quantachrome, USA). The secondary protein structure of FDH were monitored by circular dichroism (CD, ABSCIEX-api 3000, Applied Photophysics, UK). The specific surface area and pore size distribution were calculated by the Brunauer–Emmett–Teller (BET) method. Electrochemical impedance spectroscopy (EIS, Gamry) analysis was performed in the frequency range of 10^5 to 0.1 Hz at a bias potential of 0 V versus Ag/AgCl. For photocurrent-time (I-T) experiments, FTO glass was cut into 1 cm × 3 cm pieces. A 0.5 mg of NU-1006 or CNMV-NU-1006 was mixed with 100 μL of Nafion solution (1% Nafion in distilled water) and drop-casted on the exposed area (1 cm × 1 cm) of the FTO electrode. The resulting electrode was air-dried and used as working electrode for electrochemical measurements. For the detection and quantification of formate, aliquots at various time points were taken and analyzed for formate concentration by using a Shimadzu 2010 Plus gas chromatograph mass spectrometry (GC-MS) with a Rtx-5MS column (30 m × 0.25 mm × 0.25 μm). The column oven temperature and injection temperature of GC are 40 ℃ and 220 ℃, respectively. And the temperature rise procedure is maintained at 40 ℃ for 3 min, and then rise it at 10 ℃ per min to 280 ℃, and finally maintained for 5 min. The ion source temperature and interface temperature of MS are 200 ℃ and 280 ℃, respectively.

FITC-labeled FDH for confocal laser scanning microscopy (CLSM)

6mg FDH was dissolved in 1mL PBS (7.0), and 10mg FITC in 1mL DMF. Then, 10 μ L FITC solution was added into FDH solution, and the mixture incubate at 37 ℃ for 1 h. The resulting solution was dialyzed in a dialysis bag (molecular weight =10000) until FITC could not be detected by the dialysate. Finally, 5.0 mg of CNMV-NU-1006 was dissolved in the above solution for 3 h at room temperature to ensure that FITC-labeled FDH enter the cavity of the MOF, and then the FITC-FDH@CNMV-NU-1006 was measured to know spatial location of the fluorophore-tagged biomolecules in the MOF using the confocal laser scanning microscopy (CLSM) technique.

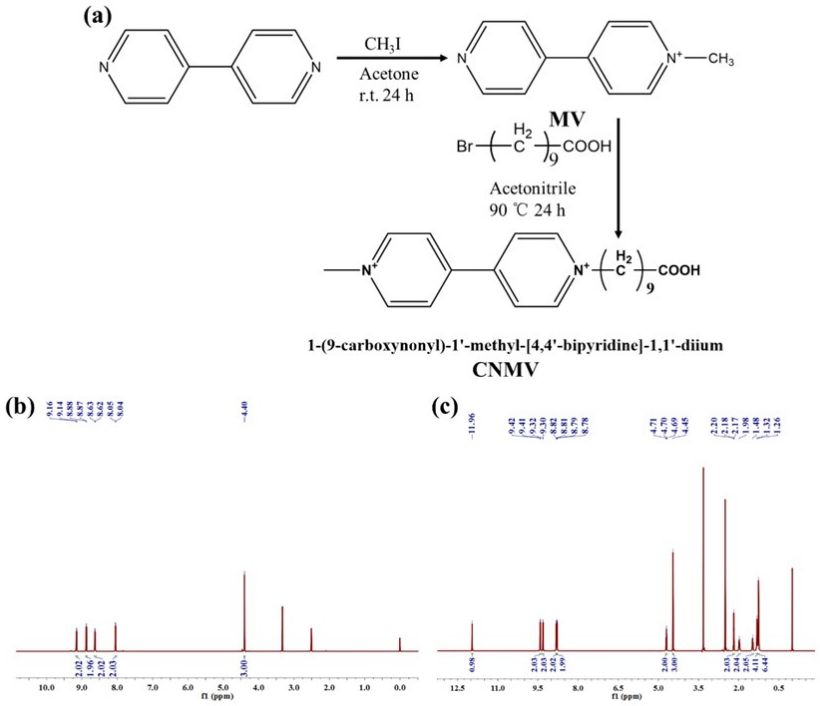

Fig. S1 (a) Synthesis route of CNMV; ^{1}H-NMR spectra of MV (b) and CNMV (c).

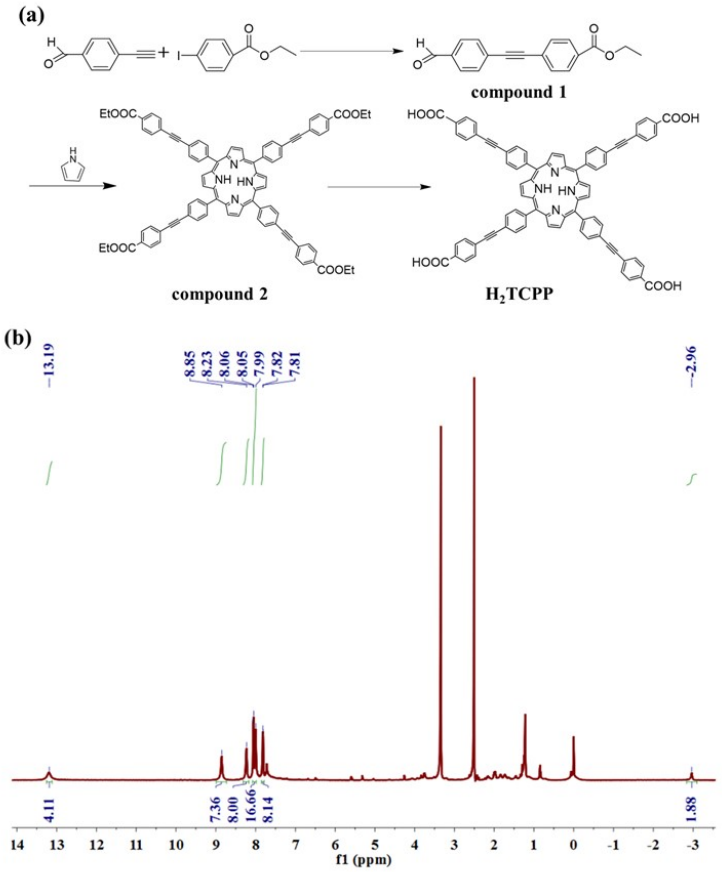

Fig. S2 (a) Schematic diagram of H_2TCPP synthesis, (b) ^1H-NMR spectra of H_2TCPP.

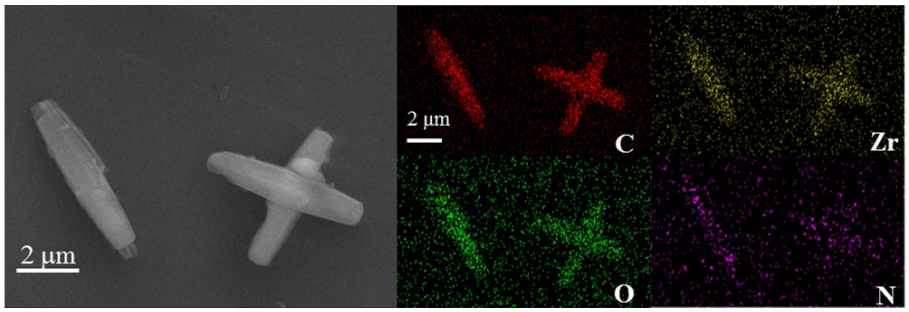

Fig. S3 SEM image of NU-1006 and corresponding SEM-EDS elemental mapping images of C, Zr, O, and N.

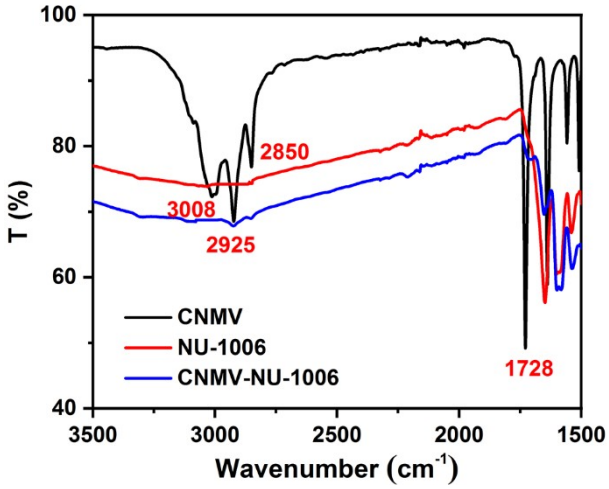

Fig. S4 FT-IR spectra of CNMV, NU-1006 and CNMV-NU-1006.

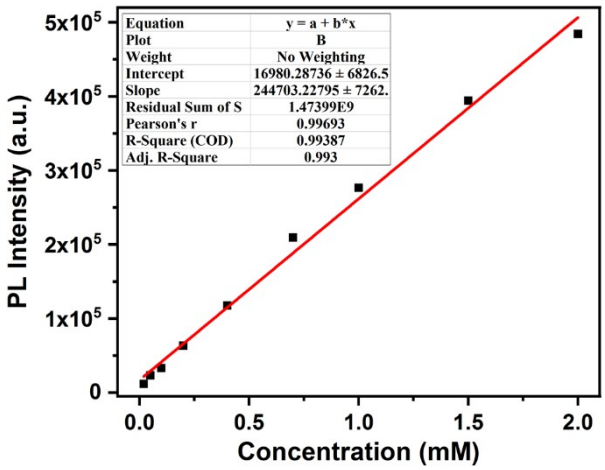

Fig. S5 Standard curve of PL intensity of CNMV versus its concentration.

After CNMV reacted with NU-1006, the product was centrifuged and washed until there was no CNMV. The supernatant was collected and the quantity of CNMV was measured using PL spectrum.

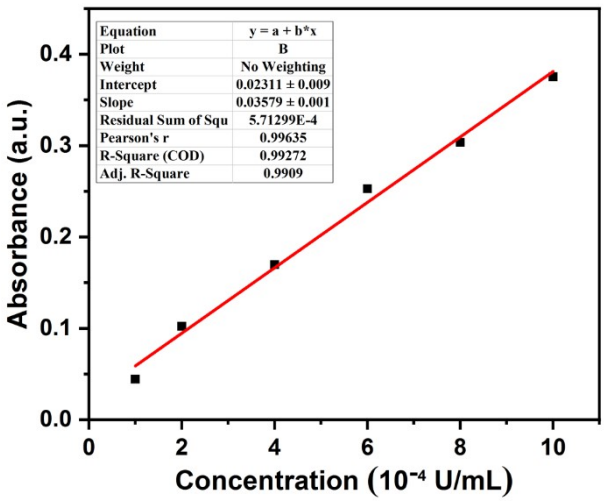

Fig. S6 Standard curve of UV-vis absorbance of NADH versus concentration of FDH.

After the incubation FDH with CNMV-NU-1006 for 3h. The solid sample was obtained by centrifugation and washed repeatedly with Tris-buffer. All the supernatants were collected and combined to regenerate the NADH. The quantity of unencapsulated FDH was determined using the standard curve in Fig. S6.

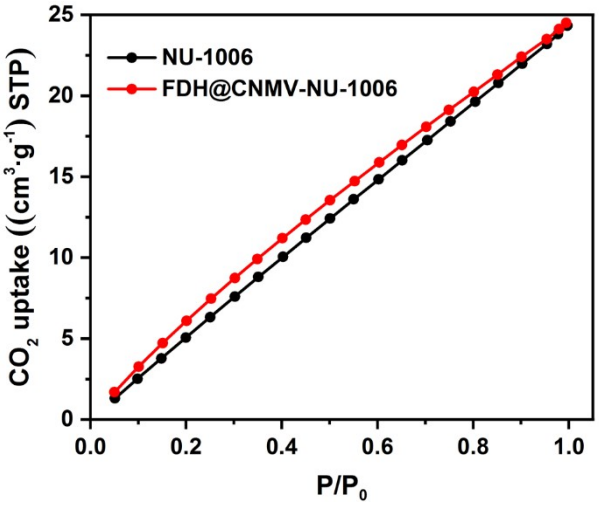

Fig. S7 CO_2 adsorption isotherms (273 K) of the as-synthesized NU-1006 and FDH@CNMV- NU-1006.

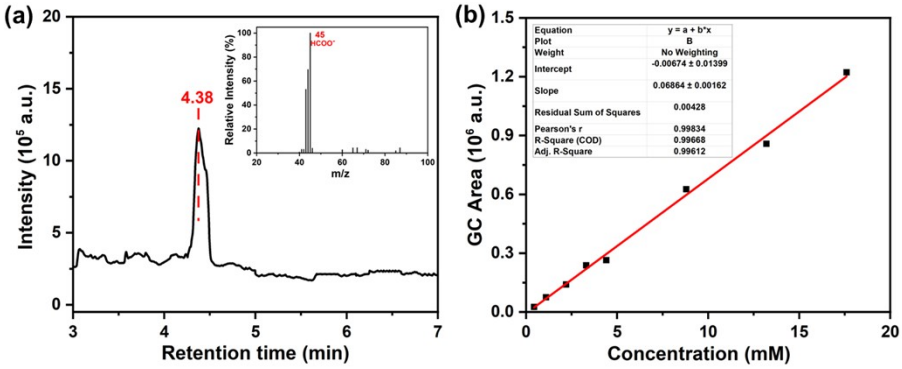

Fig. S8 (a) A representative GC-MS diagram for measuring the product (inset: the MS diagram corresponding to the peak at the retention time of 4.38 min); (b) Standard curve of peak area of formate measured by GC-MS versus its concentration.

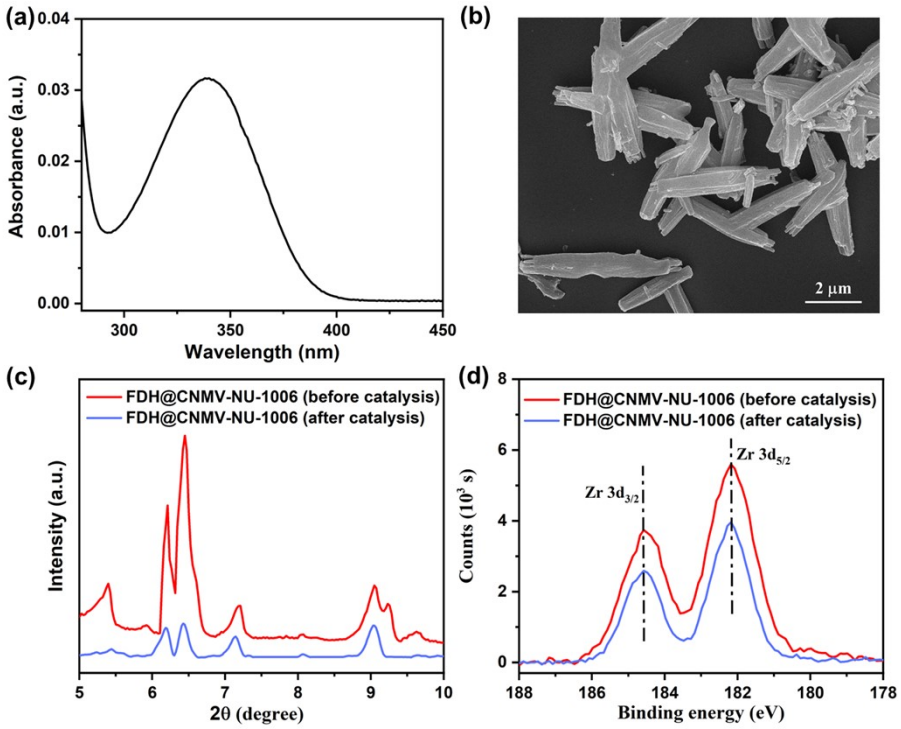

Fig. S9 (a) The detection of FDH of the reaction solution after photocatalytic experiment by regeneration of NADH; SEM image (b), SAXRD pattern (c) and XPS spectrum (d) of FDH@CNMV-NU-1006 after the 6th cycle of catalysis.

In Fig. S9a, after 6th run of photocatalysis using FDH@CNMV-NU-1006, the supernatant was collected. And 0.1 mL supernatant was incubated with NAD^+ at 37 °C for 10 min, then the absorbance of NADH was measured by UV-vis. The result indicated that 0.15 U FDH was leaked into the reaction solution.

Scanning electron microscope image of FDH@CNMV-NU-1006 after the reaction shows that its architecture remains to be intact (Fig. S9b). The XRD peaks are retained after reaction as well though there is slight decrease of the intensity (Fig. S9c). The refined Zr 3d XPS spectrum of FDH@CNMV-NU-1006 doesn't show any shift of the binding energy (Fig. S9d). All the above results disclose that FDH@CNMV-NU-1006 is stable after 6 runs of photocatalytic reaction.

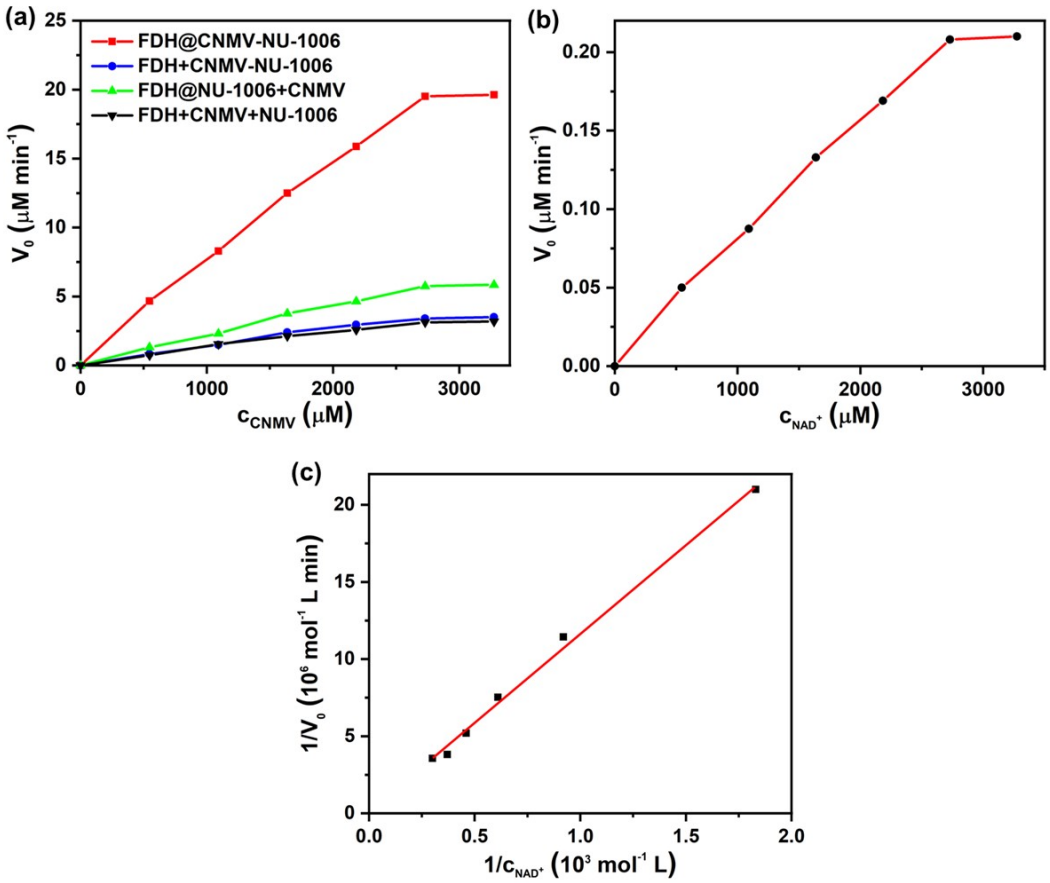

Fig. S10 (a) Initial formate generating rate versus the concentration of CNMV; (b) Initial formate generating rate versus the concentration of NAD^+; (c)Lineweaver–Burk plot for formic acid production rate of FDH with the concentration of NAD^+.

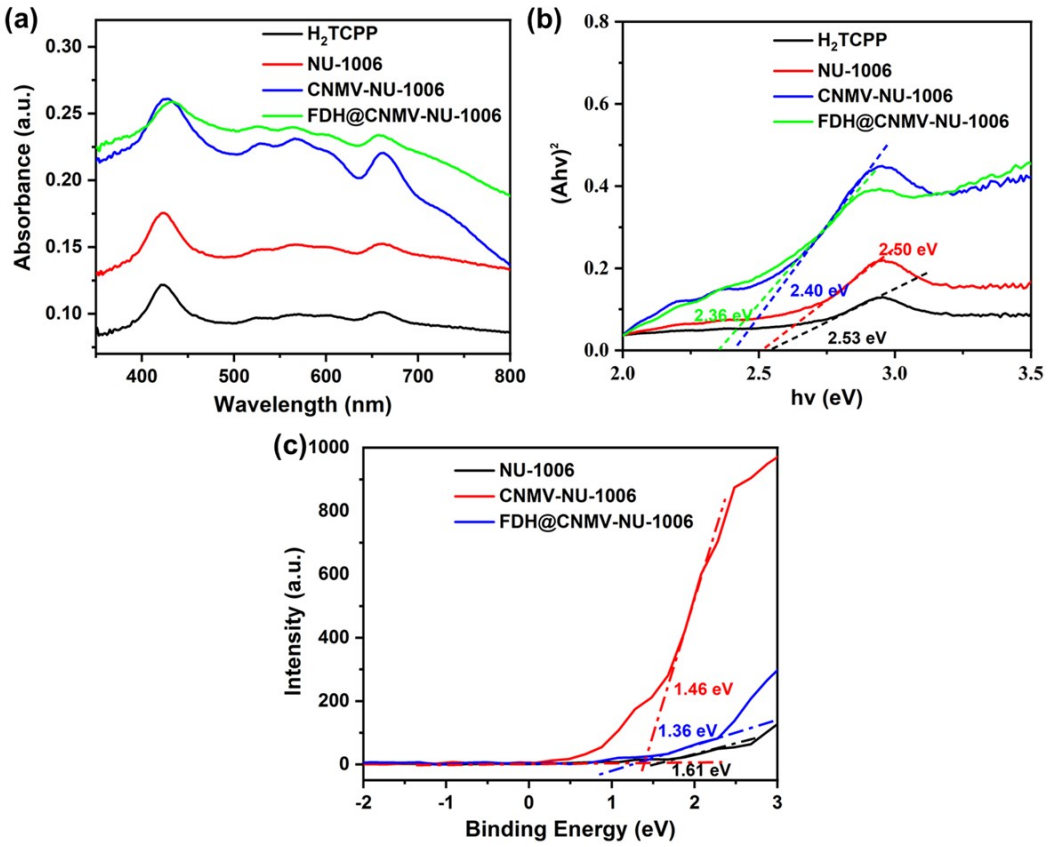

Fig. S11 (a) UV-vis diffuse reflection spectra of H_2TCPP, NU-1006 and CNMV-NU-1006; (b) Bandgap estimated from the Kubelka–Munk equation according to UV-vis diffuse reflection spectra; (c) Valence band obtained from XPS.

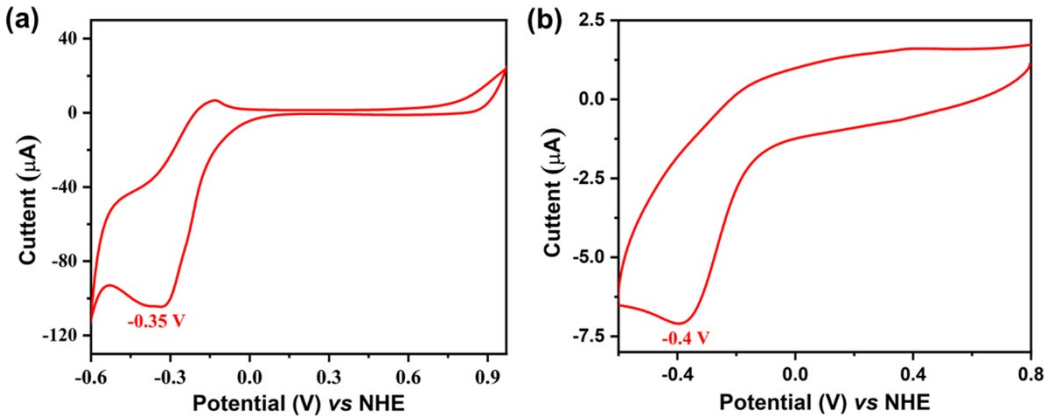

Fig. S12 Cyclic voltammogram of CNMV (a) and Zr Cluster (b) at a scan rate of 0.1 V/s (*vs* NHE).

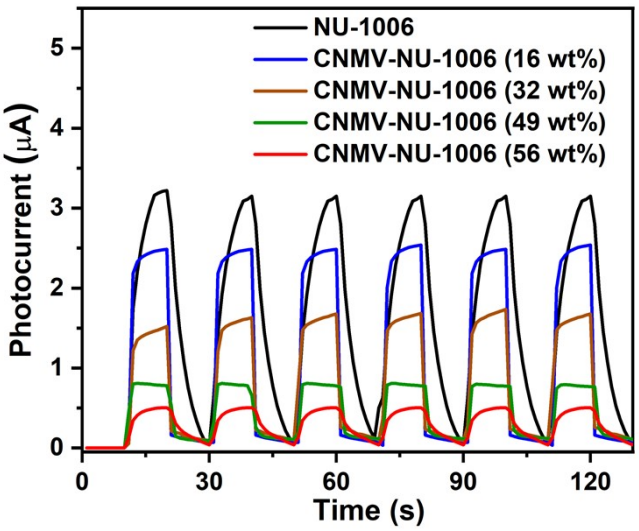

Fig. S13 Photocurrent-time profiles of NU-1006, CNMV-NU-1006 (16 wt %), CNMV-NU-1006 (32 wt %), CNMV-NU-1006 (49 wt %) and CNMV-NU-1006 (56 wt %) at the potential of 0 V *vs.* NHE.

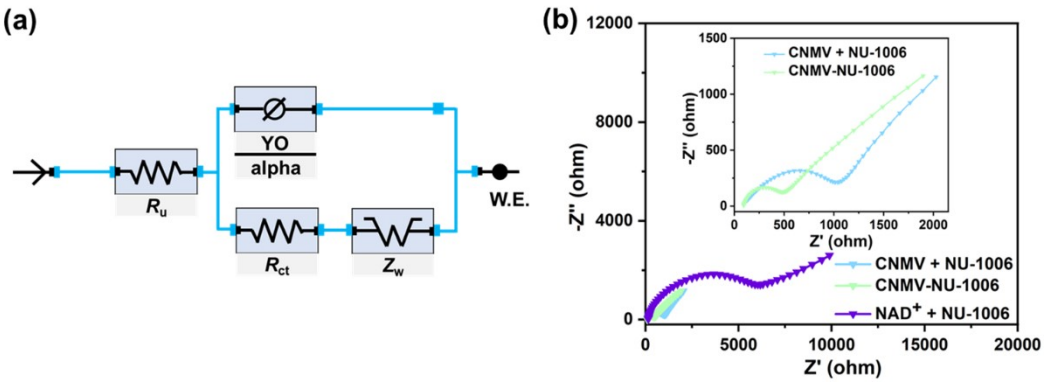

Fig. S14 (a) Equivalent circuit diagram of EIS; (b) Nyquist plots of the EIS data of CNMV+NU-1006, CNMV-NU-1006 and NAD^++NU-1006 (inset: CNMV+NU-1006 and CNMV-NU-1006).

Table S1 Comparison of the performance of NAD^+ and MV derivatives mediated CO_2 photoreduction.

NAD^+	Formate (μ mol U^{-1} h^{-1})	TOF	Ref.	MV^{2+} derivatives	Formate (μ mol U^{-1} h^{-1})	TOF	Ref.
NAD^+ (0.10 mM), EY (2.0 μM), and TEOA (400 mM)	5.42	28.33 h^{-1} (in 48 h)	1	TEOA (0.3 M), ZnTPPS (10 mM), BP (100 mM), FDH (6.4 μM), PBS 5.0 ml of 10 mM	0.123	18.8 h^{-1} (in 1 h)	7
20 mL Tris-HCl buffer (0.05 M, pH 7), 1 mM NADH, 7 mg FDH	0.62	3.73 h^{-1} (in 6 h)	2	40 mM MV^{2+}, 2.6 μM FDH, 7.5 mL buffer solution	0.21	75 h^{-1} (in 2 h)	8
PBS (0.1 M, pH 6.0), NADH (1 × 10^{-3} M), FDH (1 mg mL^{-1})	0.0007	0.03 h^{-1} (in 24 h)	3	TEOA (0.3 M), TiO_2 NP (6.8 mg•L^{-1}), MV (0.5 mM), FDH (7.5 μM)	0.16	10.13 h^{-1} (in 2 h)	9
NAD^+ (1 mM), PBS (100 mM, pH = 7), TEOA (15 w/v%), MAF-7@FDH (7.5 mg), TPE-	0.93	1.86 h^{-1} (in 9 h)	4	10 mM MV, 10 μM FDH, 100 mM PBS (8.0)	0.125	9.38 h^{-1} (in 10 min)	10

C_3N_4/PEI/Rh (3 mg)							
CbFDH (2 g L^{-1}), TEOA (100 mM), PBS buffer (pH 7.0, 100 mM)	0.5	62.01 h^{-1} (in 1 h)	5	TEOA (1.5 mM), ZnTPPS (50 nM), ACBP (0.5 mM), FDH (5.3 nmol), 5.0 ml PBS	0.0283	1.7 h^{-1} (in 1 h)	11
Graphene-Based photocatalyst (0.5 mg), β-NAD (1.24 m mol), Rh (0.62 µmol), FDH (3 U), PBS (100 mM, pH 7.0, 3.1 mL), TEOA (1.24 mmol)	0.0184	1.69 h^{-1} (in 2 h)	6	FDH (1 U/mL), Tris-buffer (3 mL, 50 mM), TEOA (0.5 mM)	1.17	75.51 h^{-1} (in 8 h)	This work

Table S2 Kinetic parameters for CO_2 to formic acid conversion with different coenzyme and FDH.

	V_{max} (mM min^{-1})	K_m (mM)	k_{cat} (min^{-1})	k_{cat}/K_m (m M^{-1} min^{-1})
FDH@NU-1006+NAD^+	0.012	167.85	0.6	0.003
FDH+CNMV+NU-1006	0.015	10.31	0.97	0.094
FDH@NU-1006+CNMV	0.015	9.39	0.97	0.1
FDH+CNMV-NU-1006	0.026	10.32	1.68	0.16
FDH@CNMV-NU-1006	0.06	6.72	3.87	0.57

Table S3 Fitting parameters of PL decay curves for H_2TCPP, H_2TCPP mixed with CNMV, NU-1006, NU-1006 mixed with CNMV and CNMV-NU-1006.

Sample	τ1/ns (rel.%)	τ2/ns (rel.%)	τ/ns	k_{ET} (10^8 s^{-1})
H_2TCPP	17.27 (7.06)	8.76 (92.94)	9.07	
H_2TCPP+CNMV	2.54 (4.31)	9.50 (95.69)	8.50	0.074
NU-1006	1.04 (4.84)	9.81 (95.16)	6.96	0.33
CNMV+NU-1006	1.24 (17.65)	1.05 (82.35)	4.52	1.11
CNMV-NU-1006	1.26 (22.45)	1.01 (77.55)	3.94	1.44

References

1 P.T. Fard, S.K. Albert, J. Ko, S. Lee, S.J. Park, J. Kim, *ACS Cat.*, 2022, **12**, 9698−9705.

2 M. Chai, S.R. Bazaz, R.Daiyan, A. Razmjou, M.E.Warkiani, R. Amal, V. Chen, *Chem. Eng. J.*, 2021, **426**, 130856.

3 S.Y. Lee, S.Y. Lim, D. Seo, J.Y. Lee, T.D. Chung, *Adv. Energy Mater.*, 2016, **6**, 1502207.

4 Y. Tian, Y.N. Zhou, Y.C. Zong, J.S. Li, N. Yang, M. Zhang, Z.Q. Guo, H. Song, *ACS Appl. Mater. Interfaces*, 2020, **12**, 34795−34805.

5 S.H. Zhang, J.F. Shi, Y.Y. Sun, Y.Z. Wu, Y.S. Zhang, Z.Y. Cai, Y.X. Chen, C. You, P.P. Han, Z.Y. Jiang, *ACS Catal.*, 2019, **9**, 3913−3925.

6 R.K. Yadav, J.O. Baeg, G.H. Oh, N.J. Park, K.J. Kong, J. Kim, D.W. Hwang, S.K. Biswas, *J. Am. Chem. Soc.*, 2012, **134**, 11455−11461.

7 S. Ikeyama, Y. Amao, *Sustain. Energy Fuels*, 2017, **1**, 1730-1733.

8 B.S. Jayathilake, S. Bhattacharya, N. Vaidehi, S.R. Narayanan, *Acc. Chem. Res.*, 2019, **52**, 676−685.

9 T. Ishibashi, S. Ikeyama, M. Ito, S. Ikeda, Y. Amao, *Chem. Lett.*, 2018, **47**, 1505-1508.

10 S. Ikeyama, Y. Amao, *ChemCatChem.*, 2017, **9**, 833-838.

11 A. Miyaji, Y. Amao, *New J. Chem.*, 2021, **45**, 5780-5790.